CLIMATOLOGY

Past and future rainfall in the Horn of Africa

Jessica E. Tierney,[1,2]* Caroline C. Ummenhofer,[2] Peter B. deMenocal[3]

10.1126/sciadv.1500682

The recent decline in Horn of Africa rainfall during the March–May "long rains" season has fomented drought and famine, threatening food security in an already vulnerable region. Some attribute this decline to anthropogenic forcing, whereas others maintain that it is a feature of internal climate variability. We show that the rate of drying in the Horn of Africa during the 20th century is unusual in the context of the last 2000 years, is synchronous with recent global and regional warming, and therefore may have an anthropogenic component. In contrast to 20th century drying, climate models predict that the Horn of Africa will become wetter as global temperatures rise. The projected increase in rainfall mainly occurs during the September–November "short rains" season, in response to large-scale weakening of the Walker circulation. Most of the models overestimate short rains precipitation while underestimating long rains precipitation, causing the Walker circulation response to unrealistically dominate the annual mean. Our results highlight the need for accurate simulation of the seasonal cycle and an improved understanding of the dynamics of the long rains season to predict future rainfall in the Horn of Africa.

INTRODUCTION

During the last 30 years, the Horn of Africa has experienced a persistent decline in rainfall during the March-April-May (MAM) "long rains" season, the primary rainy season for the region (*1*–*3*). This has had major consequences for regional food security, where agriculture largely depends on rainfall and is thus highly vulnerable to climatic change (*1*, *4*). It is unclear whether this decline is caused by internal multidecadal variability associated with changes in the tropical Pacific (*3*–*5*) or anthropogenically driven warming in the Indian Ocean or western Pacific region (*1*, *2*, *6*–*8*). Yet, thus far, the decline has only been analyzed within the context of sparse and short regional climatological data. Establishing whether this drying trend is unusual, and therefore possibly anthropogenically caused, requires past climate information that extends beyond the instrumental record. Here, we present a detailed record of changes in regional temperature and aridity in the eastern Horn of Africa region (Somalia, Djibouti, and eastern Ethiopia) spanning the last 2000 years, which places the recent drying in a historical context. We then juxtapose the paleoclimate information with climate simulations conducted as part of the recent Coupled Model Intercomparison Project 5 (CMIP5, http://cmip-pcmdi.llnl.gov/cmip5/) and discuss the implications for future prediction of regional aridity.

Natural archives of climate change in the eastern Horn of Africa region are limited—there are no permanent lake basins, few trees, and no high-altitude ice cores. However, the nearby Gulf of Aden contains organic-rich sediments that accumulate sufficiently quickly to allow for recent paleoclimate reconstruction (*9*). For this study, we generated a high-resolution paleoclimate record based on data derived from two overlapping marine cores (Fig. 1A). Relatively high accumulation rates at our core site (0.05 to 0.1 cm/year, see the Supplementary Materials) allow for a decadal resolution time series of both marine and terrestrial climate. To reconstruct past changes in sea surface temperature (SST), we used the TEX_{86} (tetraether index of 86 carbons) proxy, which is based on the relative cyclization of marine archaeal glycerol dialkyl glycerol tetraethers, and a Bayesian calibration that improves the accuracy of regional predictions (see the Supplementary Materials) (*10*). To reconstruct aridity, we measured the hydrogen isotopic composition of leaf waxes (δD_{wax}). δD_{wax} is a faithful indicator for past changes in aridity in Africa (*11*), with more positive (negative) values corresponding to arid (wet) conditions (*9*, *12*, *13*). Leaf waxes are primarily transported from the eastern Horn of Africa to the Gulf of Aden by aeolian processes, providing a comprehensive view of average aridity in the eastern Horn and Afar regions (see the Supplementary Materials) (*9*).

RESULTS

Figure 1B presents the proxy data from the Gulf of Aden. Before the 20th century, SSTs in the region varied within 1.5°C, with the first millennium (150–1050 AD) on average slightly (0.2°C) warmer than the second millennium (1050–1850 AD). TEX_{86} indicates that regional SSTs rose by ca. 0.8°C between the late 1800s and 2001, in good agreement with observational estimates (fig. S5). Given the calibration errors associated with the TEX_{86} proxy, we cannot assess whether the current SSTs are unprecedented in the last 2000 years, but the rapid 20th century rise is unique in the context of past variability (Fig. 1B). Overall, the TEX_{86}-based SST record gives a clear picture of how temperatures near the Horn of Africa have changed in the recent past. Notably, we find that there have been only minimal changes in surface temperatures before the most recent warming. There is no indication of a warm period associated with the Northern Hemisphere Medieval Warm Period (ca. 1000–1400 AD) or a cool period associated with the Little Ice Age (LIA, ca. 1450–1800).

The δD_{wax} data indicate that regional aridity has changed more substantially than temperature in the past few millennia (Fig. 1C). Unlike the TEX_{86} data (Fig. 1B), the δD_{wax} data follow the trajectory of Northern Hemisphere temperatures with warm temperatures corresponding to drier conditions, and cold temperatures, corresponding to wetter conditions (Fig. 1C). Given the known influence of western Indian Ocean SSTs on the East African short rains (*8*, *14*), the fact that the δD_{wax} record follows Northern Hemisphere temperatures, rather than our local TEX_{86}-based SST record, may indicate that changes in long rains season precipitation (during which time the relationship to western Indian Ocean SSTs is weak) dominate the recent paleoclimate record. Alternatively, the differences between the TEX_{86} record and Northern

[1]Department of Geosciences, The University of Arizona, Tucson, AZ 85721, USA. [2]Woods Hole Oceanographic Institution, Woods Hole, MA 02540, USA. [3]Lamont Doherty Earth Observatory, Palisades, NY 10964, USA.
*Corresponding author. E-mail: jesst@email.arizona.edu

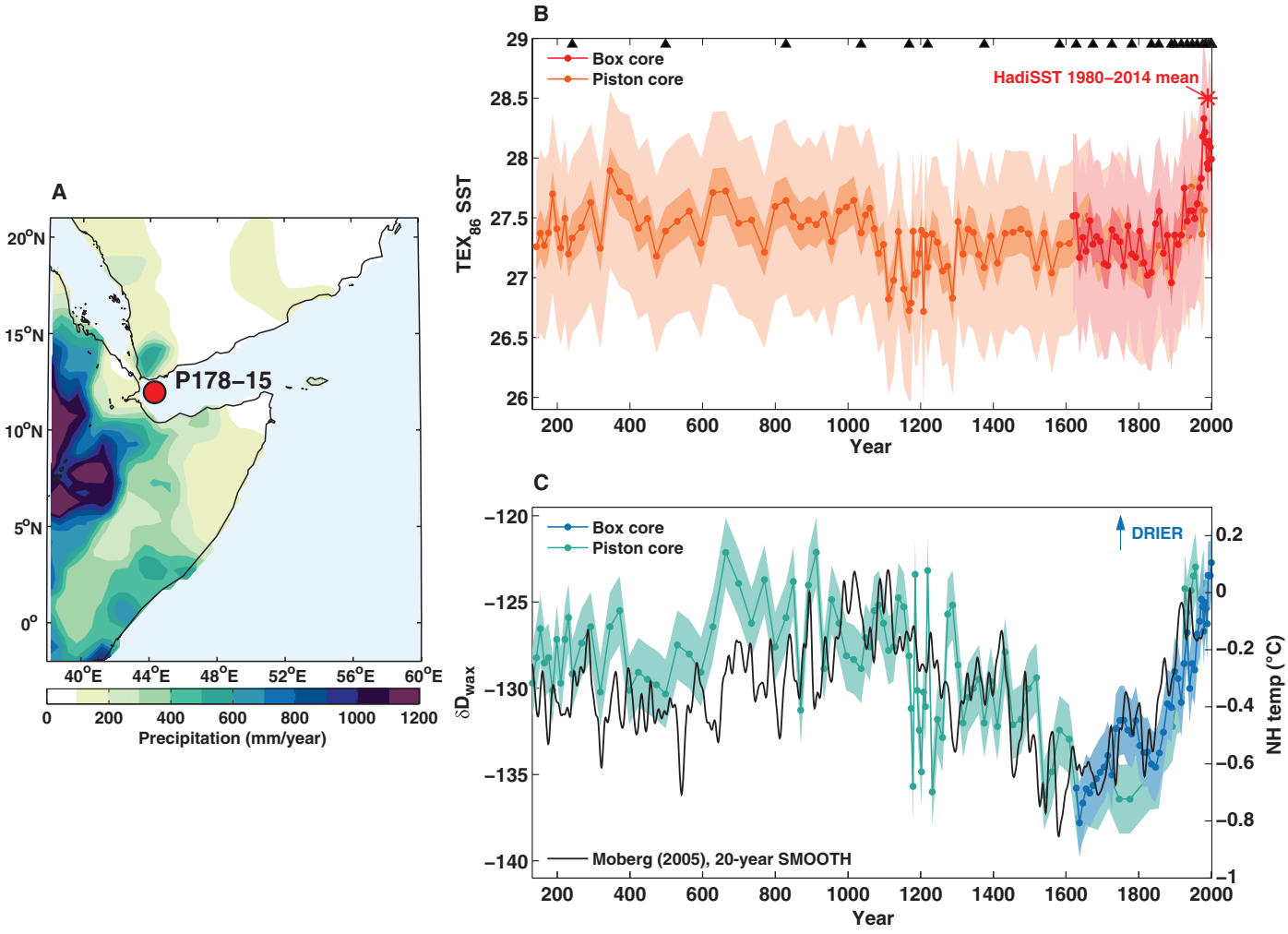

Fig. 1. Temperature and aridity proxy data from marine core site P178-15 in the Gulf of Aden. (**A**) Location of site P178-15 and annual average precipitation in the eastern Horn of Africa region [GPCC (Global Precipitation Climatology Centre) v6 product (*39*)]. (**B**) TEX_{86}-inferred SSTs (in degrees Celsius) for the past two millennia from the box core (in red) and piston core (in orange) at site P178-15. Darker error bars denote the 1σ analytical error, and lighter error bars denote the 1σ calibration error using the BAYSPAR-NRS calibration model (*10*). Black triangles denote intervals where the cores were dated with either ^{14}C or ^{210}Pb. The red star indicates modern mean annual SSTs near the core site (*40*). (**C**) δD_{wax} data for the past two millennia from the Gulf of Aden cores, overlaid with a reconstruction of Northern Hemisphere (NH) temperatures (*41*). Error bars denote the 1σ analytical error. More negative (positive) values indicate wetter (drier) conditions.

Hemisphere temperatures may simply be due to local variability in the Gulf of Aden that has little influence on eastern Horn of Africa rainfall.

The wettest period of the last 2000 years occurred during the LIA. This "Little Ice Age Pluvial" is seen in other proxy records from easternmost equatorial Africa (*15*, *16*), whereas locations farther to the west near the East African Rift Lakes were dry during the LIA (*17*, *18*). These data, together with our new record from the eastern Horn region, reinforce the view that the response of East African hydroclimate to LIA cooling was the development of a coastal-interior, wet-dry dipole (*19*).

Following this wet period, δD_{wax} rose sharply, indicating increasingly arid conditions toward the present day (Fig. 1C). Although transport and sedimentation processes, especially fluvial processes, can in some cases substantially delay the delivery of leaf waxes to marine sediments (*20*), carbon isotope measurements on the Gulf of Aden leaf waxes show a pronounced decline in the 20th century—a clear evidence of the Suess effect (Fig. 2 and see the Supplementary Materials), indicating that the aeolian-dominated transport in this region is sufficiently rapid to preserve 20th century trends. The rise in δD_{wax} is therefore contemporary, and although the values of δD_{wax} achieved by the end of the 20th century are not unprecedented in the context of the last 2000 years, the rate of change is unusual (fig. S6). The coeval rise in global temperatures and δD_{wax} during the last 150 years is a continuation of the close association between eastern Horn of Africa aridity and global temperatures that has persisted over the past 2000 years; clearly, aridity in this region evolves with the state of the global climate. Because the most recent rise in global temperature can be attributed to greenhouse gas emissions (*21*), and aridity rapidly increases during this time, we infer that there is an anthropogenic component to the 20th century drying.

Although the relative paucity of instrumental data across the eastern Horn region limits the analysis of historical 20th century trends, available observations support the proxy record in suggesting an overall drying of the region (Fig. 3A). On a mean annual basis, parts of the

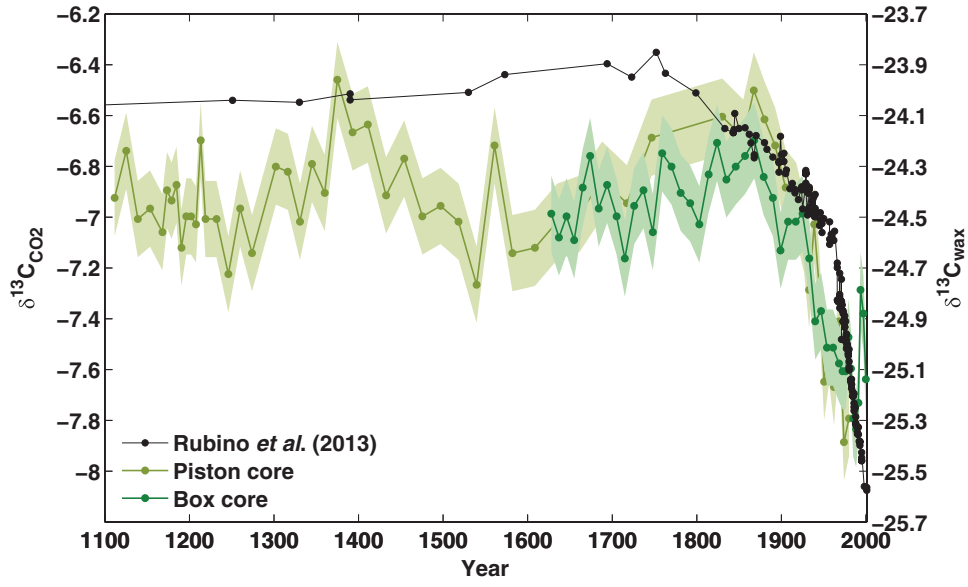

Fig. 2. $\delta^{13}C$ of leaf waxes ($\delta^{13}C_{wax}$) in the Gulf of Aden core for the past ca. 900 years (in green) versus the change in atmospheric CO_2 $\delta^{13}C$ (*42*). Note that although the absolute values are different, the relative scales are equivalent. The recent decrease in $\delta^{13}C_{wax}$ resembles the record of atmospheric CO_2 $\delta^{13}C$ both in timing and in magnitude, indicating that $\delta^{13}C_{wax}$ records the Suess effect.

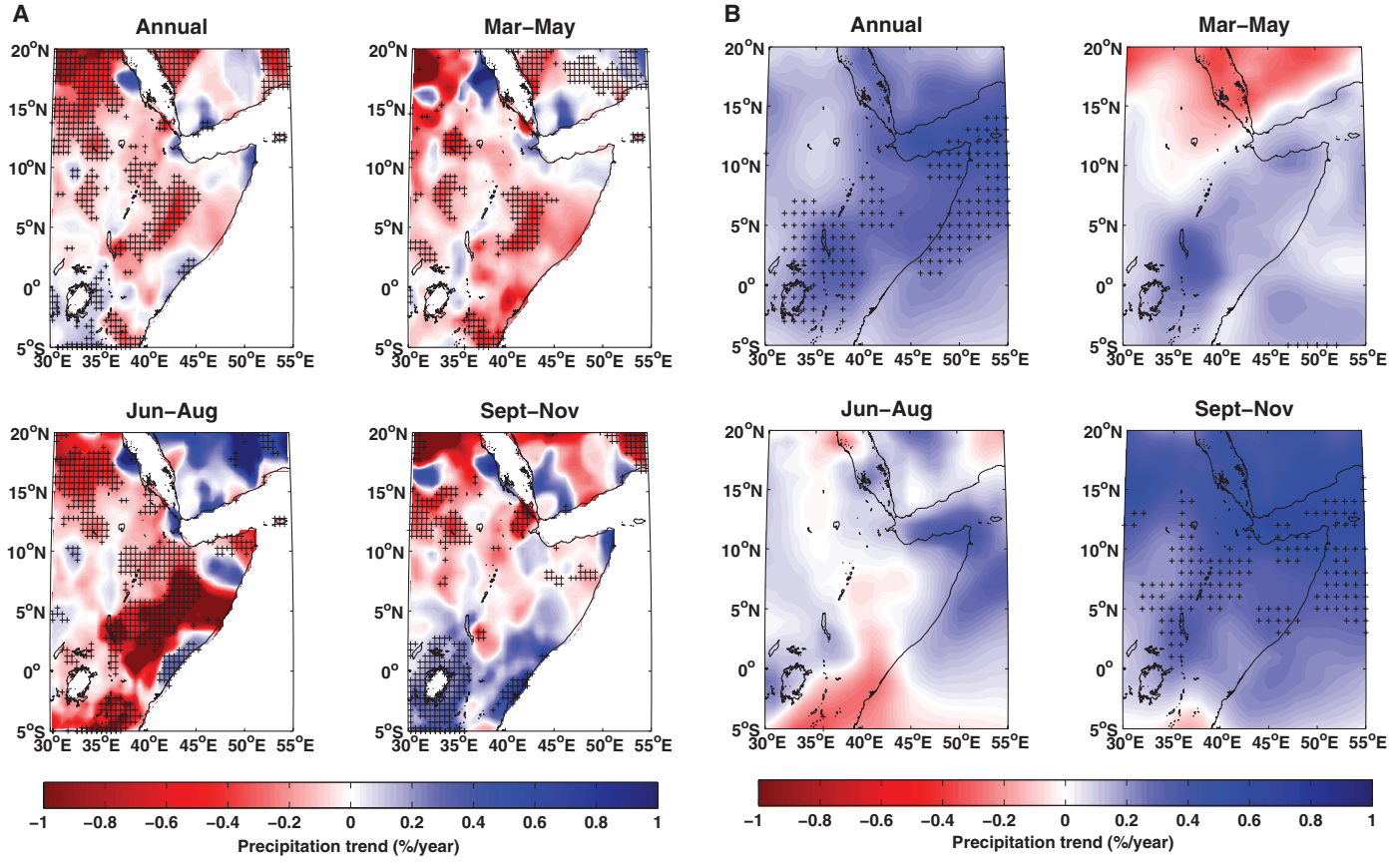

Fig. 3. Trends in 20th century observed versus 21st century simulated precipitation in the eastern Horn of Africa region. (**A**) Trends (percent per year) in observed precipitation across the 20th century [1901–2010; GPCC v6 product (*39*)], including the annual mean, the two major rainy seasons (March–May and September–November), and the dry season (June–August). Stippling indicates that the trend is significant at $P < 0.05$ (Mann-Kendall test). (**B**) Multimodel mean (model $n = 23$) of trends (percent per year) in simulated precipitation in the CMIP5 RCP 8.5 scenario for the 21st century (2006–2099). Panels as in (A). Stippling indicates areas where at least 90% of the models agree on the sign of change.

eastern Horn of Africa region have experienced less rainfall, with the reductions mainly occurring in the long rains (MAM) season and June-July-August (JJA) dry season (Fig. 2A). During the short rains [September-October-November (SON)] season, there has been a slight increase in rainfall centered near the Great Lakes region, consistent with previous assessments (Fig. 2A) (*8*, *22*).

Climate models participating in the previous Coupled Modeling Intercomparison Project 3 (CMIP3) assessment generally predicted that the greater East Africa region will become wetter in response to future increases in greenhouse gases (*23*, *24*). This contradicts the paleoclimate data presented here, which clearly suggest that future warming should be associated with drying, at least in the eastern Horn of Africa. To understand this discrepancy and identify mechanisms that affect future climate specifically in the eastern Horn region, we analyze both historical (1850–2005) and future (2006–2100) climate simulations conducted as part of CMIP5. We find that simulations of historical climate do not produce a mean annual drying trend in the Horn; rather, they suggest slightly wetter conditions on average, with an increase in both the short and long rains (fig. S7). However, there is relatively low model agreement regarding these changes (ca. 60%, see the Supplementary Materials), suggesting that in the historical model simulations, internal variability dominates over a forced response. In contrast, the paleoclimate data strongly suggest a forced response during the 20th century (Fig. 1C).

The difference between the paleoclimate data and the historical model simulations may indicate that the models are missing an important component of the regional climate response, but could also merely reflect low model sensitivity to the relatively small changes in radiative forcing across the 20th century. To more clearly understand and identify the simulated response of eastern Horn of Africa precipitation to rising greenhouse gases and temperature, we investigate the climate model projections under the high-emissions Representative Concentration Pathway (RCP) 8.5 scenario for the 21st century. In this case, the same set of models overwhelmingly (≥90% in some regions) predict wetter conditions as greenhouse gases and global temperatures rise, both seasonally and in the annual mean (Fig. 3B).

We find that this projected change in eastern Horn of Africa precipitation is associated with a weakening in the Walker Circulation over the Indian and Pacific ocean basins. Anomalously rising air in the western Indian Ocean and central Pacific regions and descending air over the Maritime continent results in increased precipitation in the eastern Horn region (Fig. 4A), similar to what occurs during interannual El Niño and positive Indian Ocean dipole (IOD) events (*14*, *25*). Over the 21st century, the slowing of the Walker Circulation causes this pattern to be more persistent, driving a long-term moistening trend in the eastern Horn of Africa in the climate models (Fig. 4A). These changes in atmospheric circulation are coupled to the surface ocean and associated with increased warming in the western Indian and central and eastern Pacific oceans relative to the Maritime region (Fig. 4B).

In agreement with previous analyses of multidecadal influences on East African rainfall in general circulation models (*19*), it is specifically the dynamical changes in the Indian Ocean basin, and not the Pacific, that cause increased rainfall in the eastern Horn of Africa in the simulations. This is evidenced by the fact that the simulated change in Horn of Africa precipitation scales with the simulated increase in the Indian Ocean west-east gradient, but not with the simulated increase in the Pacific Ocean east-west gradient (see the Supplementary Materials and fig. S8). The coupling between Indian Ocean climatology and eastern Horn of Africa rainfall is strongest during the short rains (SON) season (fig. S8), when interannual IOD events have their greatest effect

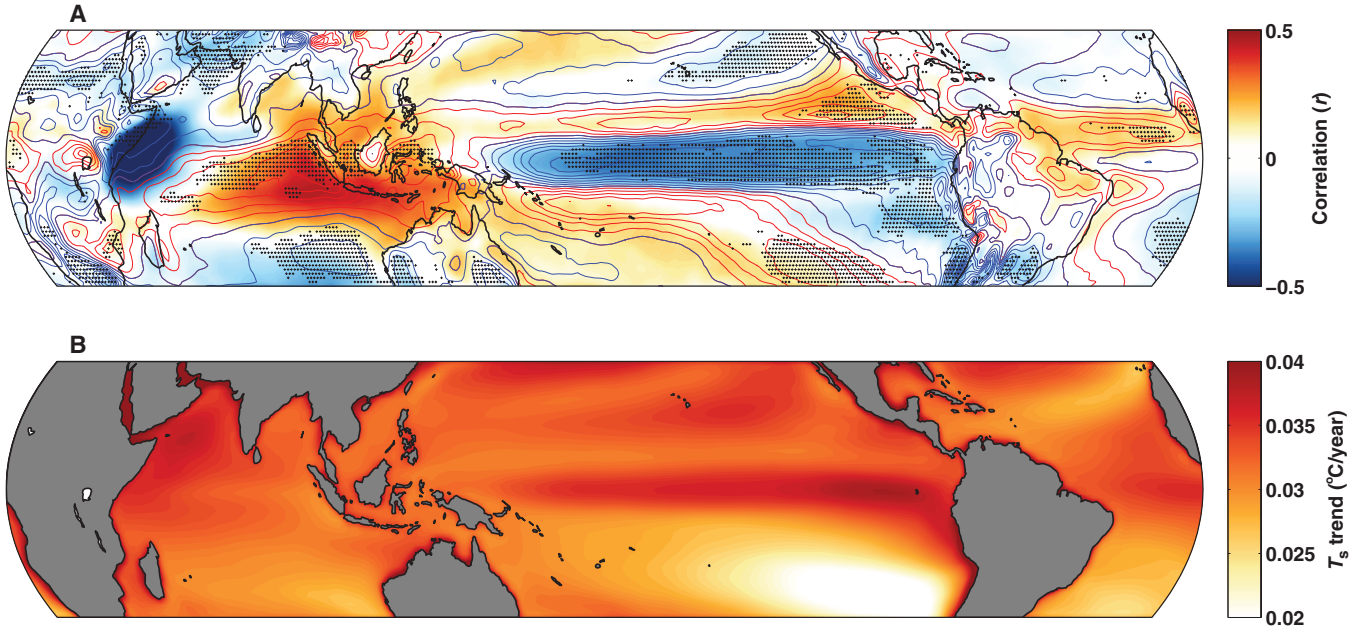

Fig. 4. Simulated 21st century changes (from the RCP 8.5 scenario) in mean annual 700 mbar vertical velocity and skin temperature in the tropics and their relation to Horn of Africa rainfall. (**A**) Multimodel mean of the correlation between eastern Horn of Africa rainfall (average across 0–12°N and 40–55°E) and 700 mbar vertical velocity (colors) and the trend in 700 mbar vertical velocity (contours). Red contours indicate a positive trend; blue contours, a negative trend. Stippling indicates areas where 90% of the models agree on the sign of the trend. (**B**) Multimodel mean of the trend in skin temperature (T_s, effectively SST) over the tropical oceans.

on East African climatology, and in turn dominates the annual mean (fig. S8).

DISCUSSION

The models predict that the "El Niño–like" Walker Circulation response to global warming will cause an increase in rainfall over the eastern Horn of Africa, primarily during the short rains season. This is a fundamentally different pattern from what the proxy record and 20th century observations indicate; the latter clearly show that decreased rainfall in the long rains and dry seasons overwhelms any increases in the short rains, resulting in 20th century drying, and our new paleoclimate record indicates a close association between globally warm conditions and drying in the eastern Horn of Africa during the past 2000 years.

The dominance of the short rains response to a weakening Walker Circulation in the model simulations can be understood as a product of the limitations of the models' ability to simulate regional climate and the magnitude of the projected changes in Indo-Pacific climatology. Regarding the simulation of regional climate, the CMIP5 models poorly reproduce the seasonal cycle in rainfall in East Africa in general (*5*) and in the eastern Horn of Africa in particular (Fig. 5). Most of the models greatly overestimate short rains precipitation while underestimating, or in some cases entirely missing, the long rains season (Fig. 5). Thus, the short rains dynamics dominate the annual mean response to an unrealistic degree. For some models, the overestimation of the short rains may be related to an overly strong IOD (*26*), but this is not consistently the case for the 23 models investigated here (fig. S9). However, models with a stronger IOD do have a tendency to predict wetter conditions in the RCP 8.5 scenario (fig. S10).

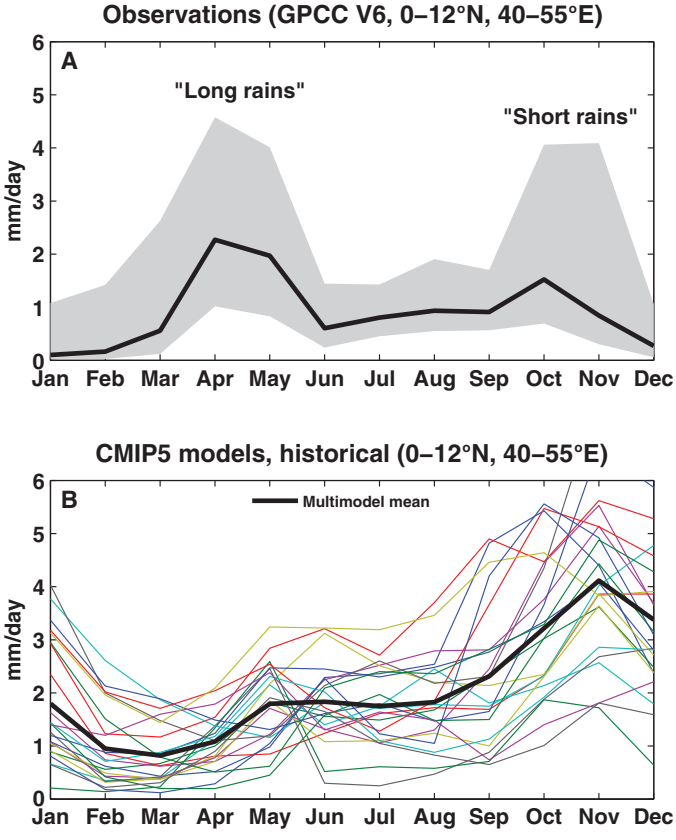

Fig. 5. Comparison between the observed and the simulated annual cycle in precipitation in the eastern Horn of Africa (average across 0–12°N and 40–55°E). (**A**) Observed annual cycle in precipitation, GPCC v6 (*39*). Black line denotes the median values; gray bars denote the 90% confidence interval. (**B**) Simulated annual cycle in precipitation, from the CMIP5 historical experiments. Black line denotes the multimodel mean; individual colored lines represent each model.

With respect to the models' Indo-Pacific climate projections, the weakening of the Walker Circulation is a common response to global warming in climate models (*27*, *28*) and dominates the predicted changes in tropical Indo-Pacific climatology in the CMIP5 simulations (Fig. 4). However, there are reasons to suspect that this predicted change is unrealistically large. For one, it is not clear that the Walker Circulation has appreciably decreased in the 20th century in spite of a notable increase in global temperatures (*29*–*33*), and the east-west SST gradient in the Pacific Ocean has actually increased (*34*, *35*). Second, although the prediction of weakening atmospheric circulation under global warming is rooted in basic physical arguments (*36*), there is some question as to whether specifically the Walker Circulation must weaken to satisfy a reduction in convective mass flux (*33*). Therefore, it is possible that the future weakening of the Walker Circulation—and associated increases in the short rains in East Africa—will be more modest than predicted.

Results from a regional climate modeling experiment focusing on Horn of Africa rainfall (*37*) lend some credence to this suspicion. Unlike the CMIP5 models, this AGCM (atmospheric general circulation model) simulation predicts increased aridity by 2050 (*37*). This experiment used ocean boundary conditions from the CMIP3 A1B scenario, including an "IOD-like" Indian Ocean SST gradient. Much like the CMIP5 model simulations investigated here, this change in the Indian Ocean gradient results in an increase in the short rains. However, this increase is much smaller than the decrease in the long rains, which arises because of a warming-related intensification of high pressure over Arabia and a shift in the Somali jet that dries the eastern Horn of Africa (*37*, *38*). Although, on average, the CMIP5 projections for the long rains indicate wetter conditions, there is more model disagreement during this season (Fig. 3B), and a few models predict substantial drying (fig. S8). These results suggest that mean annual CMIP5 model projections might be different given (i) an adequate simulation of the seasonal cycle in precipitation, (ii) a better representation of the long rains season dynamics, and (iii) a more moderate increase in short rains precipitation.

The paleoclimate data presented here give context to the recent changes in Horn of Africa aridity and alter our view of future climate change in the region. The record spanning the past two millennia indicates a persistent association between globally warm conditions and drying in the eastern Horn region, suggesting that present and future warming will be met with drying. The observed decline in rainfall during the MAM and/or JJA seasons therefore likely has an anthropogenic component, although this needs to be confirmed by detection and attribution studies. An expectation of future drying agrees with previous regional modeling work but disagrees with the predictions of the coupled climate models participating in the CMIP5 RCP 8.5 scenario. However, the model simulations may overestimate future changes in Indian and Pacific SST gradients and the associated weakening in the Walker Circulation. Furthermore, most models do not adequately simulate the seasonal cycle in rainfall and therefore overestimate the impact of increases in the short rains. As previously shown (*37*, *38*), future drying

in the eastern Horn of Africa will have a radical impact on growing season days and agriculture in the region. The large changes in aridity in the recent paleoclimate record further emphasize that low-frequency variability in East African rainfall, regardless of the origin, poses a serious threat to food security. Finally, our results highlight the need for adequate simulation of regional climatologies to properly assess the impact of global warming on subtropical arid climates.

MATERIALS AND METHODS

Paleoclimate reconstructions

We use a box core (P178-15 BC1) to reconstruct recent climate trends (ca. AD 1600 to present) and an accompanying piston core (P178-15 P) to extend the record back to ca. AD 100. These cores were collected from the Gulf of Aden at 11°57.3′N, 44°18′E, 869-m water depth from the *R/V Pelagia* in 2001. We constructed age models for these cores on the basis of a combination of ^{210}Pb and ^{14}C dating; see the Supplementary Materials for a list of dates and details concerning the age model construction. The cores were sampled at ca. 9-year resolution in the box core and ca. 20-year resolution in the piston core, with a higher sampling interval during the historical period (ca. 5 years for the box core and ca. 6 years for the piston core). For each sample, about 15 g of dried sediment was extracted and analyzed for TEX_{86} and δD_{wax}, using high-performance liquid chromatography–mass spectrometry and continuous-flow isotope ratio mass spectrometry techniques, respectively (see the Supplementary Materials for details). The TEX_{86} data were calibrated to SST using the BAYSPAR calibration model (see the Supplementary Materials for details) (*10*).

Climate model experiments

We use output from the CMIP5 modeling experiments, publicly available online at the Earth System Grid: http://pcmdi9.llnl.gov/. We use data from 23 fully coupled models participating in the "historical" experiment, which spans 1850–2005 and includes solar, orbital, greenhouse gas, and aerosol forcings in line with observed values, and the RCP 8.5 experiment, in which greenhouse gas emissions are raised across the 21st century to produce 8.5 W/m^2 of forcing by year 2100. We refer the reader to the Supplementary Materials for further details on the model simulations and analyses, including a list and description of the models used.

SUPPLEMENTARY MATERIALS

Supplementary material for this article is available at http://advances.sciencemag.org/cgi/content/full/1/9/e1500682/DC1

Materials and Methods

Table S1. ^{210}Pb dates on core P178-15 BC1.

Table S2. Radiocarbon dates on core P178-15 BC1.

Table S3. Radiocarbon dates on core P178-15P.

Table S4. List of the CMIP5 models used for the analyses.

Fig. S1. ^{210}Pb data from P178-15 BC1.

Fig. S2. The age model for P178-15 BC1.

Fig. S3. The age model for P178-15P for the last 4000 years.

Fig. S4. A sample GC-FID chromatogram of fatty acids (as methyl esters) from core P178-15P.

Fig. S5. TEX_{86}-based SST anomalies from P178-15 BC1 versus instrumental observations.

Fig. S6. First derivative of the δD_{wax} data from the Gulf of Aden.

Fig. S7. Multimodel mean of trends in simulated precipitation from the CMIP5 historical experiment.

Fig. S8. Projected change (%) in eastern Horn of Africa precipitation versus projected changes in zonal surface temperature gradients in the Indian and Pacific Ocean basins.

Fig. S9. Scatterplot of the correlation coefficient between the simulated annual cycle of precipitation in the Horn of Africa versus the observed annual cycle (from GPCC v6) and the SD of a modified Dipole Mode Index (DMI_m).

Fig. S10. Scatterplot of the SD of a modified Dipole Mode Index (DMI_m) and the projected change in precipitation for the RCP 8.5 experiment.

References (*43–74*)

REFERENCES AND NOTES

1. C. Funk, M. D. Dettinger, J. C. Michaelsen, J. P. Verdin, M. E. Brown, M. Barlow, A. Hoell, Warming of the Indian Ocean threatens eastern and southern African food security but could be mitigated by agricultural development. *Proc. Natl. Acad. Sci. U.S.A.* **105**, 11081–11086 (2008).
2. A. Williams, C. Funk, A westward extension of the warm pool leads to a westward extension of the Walker circulation, drying eastern Africa. *Clim. Dyn.* **37**, 2417–2435 (2011).
3. B. Lyon, D. DeWitt, A recent and abrupt decline in the East African long rains. *Geophys. Res. Lett.* **39**, L02702 (2012).
4. B. Lyon, Seasonal drought in the Greater Horn of Africa and its recent increase during the March–May long rains. *J. Clim.* **27**, 7953–7975 (2014).
5. W. Yang, R. Seager, M. A. Cane, B. Lyon, The East African long rains in observations and models. *J. Clim.* **27**, 7185–7202 (2014).
6. A. Park Williams, C. Funk, J. Michaelsen, S. A. Rauscher, I. Robertson, T. H. G. Wils, M. Koprowski, Z. Eshetu, N. J. Loader, Recent summer precipitation trends in the Greater Horn of Africa and the emerging role of Indian Ocean sea surface temperature. *Clim. Dyn.* **39**, 2307–2328 (2012).
7. A. Hoell, C. Funk, Indo-Pacific sea surface temperature influences on failed consecutive rainy seasons over eastern Africa. *Clim. Dyn.* **43**, 1645–1660 (2014).
8. B. Liebmann, M. P. Hoerling, C. Funk, I. Bladé, R. M. Dole, D. Allured, X. Quan, P. Pegion, J. K. Eischeid, Understanding recent Eastern Horn of Africa rainfall variability and change. *J. Clim.* **27**, 8630–8645 (2014).
9. J. E. Tierney, P. B. deMenocal, Abrupt shifts in Horn of Africa hydroclimate since the last glacial maximum. *Science* **342**, 843–846 (2013).
10. J. E. Tierney, M. P. Tingley, A Bayesian, spatially-varying calibration model for the TEX_{86} proxy. *Geochim. Cosmochim. Acta* **127**, 83–106 (2014).
11. Y. Garcin, V. F. Schwab, G. Gleixner, A. Kahmen, G. Todou, O. Séné, J.-M. Onana, G. Achoundong, D. Sachse, Hydrogen isotope ratios of lacustrine sedimentary n-alkanes as proxies of tropical African hydrology: Insights from a calibration transect across Cameroon. *Geochim. Cosmochim. Acta* **79**, 106–126 (2012).
12. E. Schefuß, S. Schouten, R. R. Schneider, Climatic controls on central African hydrology during the past 20,000 years. *Nature* **437**, 1003–1006 (2005).
13. J. E. Tierney, J. M. Russell, Y. Huang, J. S. Sinninghe Damsté, E. C. Hopmans, A. S. Cohen, Northern hemisphere controls on tropical southeast African climate during the past 60,000 years. *Science* **322**, 252–255 (2008).
14. E. Black, J. Slingo, K. R. Sperber, An observational study of the relationship between excessively strong short rains in coastal East Africa and Indian Ocean SST. *Mon. Weather Rev.* **131**, 74–94 (2003).
15. D. Verschuren, K. R. Laird, B. F. Cumming, Rainfall and drought in equatorial east Africa during the past 1,100 years. *Nature* **403**, 410–414 (2000).
16. J. E. Tierney, J. M. Russell, J. S. Sinninghe Damsté, Y. Huang, D. Verschuren, Late Quaternary behavior of the East African monsoon and the importance of the Congo Air Boundary. *Quat. Sci. Rev.* **30**, 798–807 (2011).
17. J. E. Tierney, M. T. Mayes, N. Meyer, C. Johnson, P. W. Swarzenski, A. S. Cohen, J. M. Russell, Late-twentieth-century warming in Lake Tanganyika unprecedented since AD 500. *Nat. Geosci.* **3**, 422–425 (2010).
18. J. M. Russell, T. C. Johnson, Little Ice Age drought in equatorial Africa: Intertropical convergence zone migrations and El Niño–Southern Oscillation variability. *Geology* **35**, 21–24 (2007).
19. J. E. Tierney, J. E. Smerdon, K. J. Anchukaitis, R. Seager, Multidecadal variability in East African hydroclimate controlled by the Indian Ocean. *Nature* **493**, 389–392 (2013).
20. V. Galy, T. Eglinton, Protracted storage of biospheric carbon in the Ganges-Brahmaputra basin. *Nat. Geosci.* **4**, 843–847 (2011).
21. N. L. Bindoff, P. A. Stott, K. M. AchutaRao, M. R. Allen, N. Gillett, D. Gutzler, K. Hansingo, G. Hegerl, Y. Hu, S. Jain, I. I. Mokhov, J. Overland, J. Perlwitz, R. Sebbari, X. Zhang, in *Climate Change 2013: The Physical Science Basis. Contribution of Working Group I to the Fifth Assessment Report of the Intergovernmental Panel on Climate Change*, T. F. Stocker, D. Qin, G.-K. Plattner, M. Tignor, S. K. Allen, J. Boschung, A. Nauels, Y. Xia, V. Bex, P. M. Midgley, Eds. (Cambridge Univ. Press, Cambridge, 2013).
22. M. Hulme, R. Doherty, T. Ngara, M. New, D. Lister, African climate change: 1900-2100. *Clim. Res.* **17**, 145–168 (2001).

23. J. H. Christensen, B. Hewitson, A. Busuioc, A. Chen, X. Gao, I. Held, R. Jones, R. K. Kolli, W.-T. Kwon, R. Laprise, V. Magaña Rueda, L. Mearns, C. G. Menéndez, J. Räisänen, A. Rinke, A. Sarr, P. Whetton, in *Climate Change 2007: The Physical Science Basis. Contribution of Working Group I to the Fourth Assessment Report of the Intergovernmental Panel on Climate Change*, S. Solomon, D. Qin, M. Manning, Z. Chen, M. Marquis, K. B. Averyt, M. Tignor, H. L. Miller, Eds. (Cambridge Univ. Press, Cambridge, 2007).
24. M. E. Shongwe, G. J. van Oldenborgh, B. van den Hurk, M. van Aalst, Projected changes in mean and extreme precipitation in Africa under global warming. Part II: East Africa. *J. Clim.* **24**, 3718–3733 (2011).
25. S. E. Nicholson, J. Kim, The relationship of the El Niño–Southern oscillation to African rainfall. *Int. J. Climatol.* **17**, 117–135 (1997).
26. E. Weller, W. Cai, Realism of the Indian Ocean dipole in CMIP5 models: The implications for climate projections. *J. Clim.* **26**, 6649–6659 (2013).
27. G. A. Vecchi, B. J. Soden, Global warming and the weakening of the tropical circulation. *J. Clim.* **20**, 4316–4340 (2007).
28. H. Tokinaga, S.-P. Xie, A. Timmermann, S. McGregor, T. Ogata, H. Kubota, Y. M. Okumura, Regional patterns of tropical Indo-Pacific climate change: Evidence of the Walker circulation weakening. *J. Clim.* **25**, 1689–1710 (2012).
29. G. A. Vecchi, B. J. Soden, A. T. Wittenberg, I. M. Held, A. Leetmaa, M. J. Harrison, Weakening of tropical Pacific atmospheric circulation due to anthropogenic forcing. *Nature* **441**, 73–76 (2006).
30. B. Sohn, S.-C. Park, Strengthened tropical circulations in past three decades inferred from water vapor transport. *J. Geophys. Res. Atmos.* **115**, D15112 (2010).
31. M. A. Merrifield, M. E. Maltrud, Regional sea level trends due to a Pacific trade wind intensification. *Geophys. Res. Lett.* **38**, L21605 (2011).
32. M. L. L'Heureux, S. Lee, B. Lyon, Recent multidecadal strengthening of the Walker circulation across the tropical Pacific. *Nat. Clim. Chang.* **3**, 571–576 (2013).
33. S. Sandeep, F. Stordal, P. D. Sardeshmukh, G. P. Compo, Pacific Walker Circulation variability in coupled and uncoupled climate models. *Clim. Dyn.* **43**, 103–117 (2014).
34. K. B. Karnauskas, R. Seager, A. Kaplan, Y. Kushnir, M. A. Cane, Observed strengthening of the zonal sea surface temperature gradient across the equatorial Pacific Ocean. *J. Clim.* **22**, 4316–4321 (2009).
35. C. C. Funk, A. Hoell, The leading mode of observed and CMIP5 ENSO-residual sea surface temperatures and associated changes in Indo-Pacific climate. *J. Clim.* **28**, 4309–4329 (2015).
36. I. M. Held, B. J. Soden, Robust responses of the hydrological cycle to global warming. *J. Clim.* **19**, 5686–5699 (2006).
37. K. H. Cook, E. K. Vizy, Impact of climate change on mid-twenty-first century growing seasons in Africa. *Clim. Dyn.* **39**, 2937–2955 (2012).
38. K. H. Cook, E. K. Vizy, Projected changes in East African rainy seasons. *J. Clim.* **26**, 5931–5948 (2013).
39. U. Schneider, A. Becker, P. Finger, A. Meyer-Christoffer, B. Rudolf, M. Ziese, GPCC full data reanalysis version 6.0 at 0.5°: Monthly land-surface precipitation from rain-gauges built on GTS-based and historic data (DWD, Offenbach, Germany, 2011).
40. N. A. Rayner, D. E. Parker, E. B. Horton, C. K. Folland, L. V. Alexander, D. P. Rowell, Global analyses of sea surface temperature, sea ice, and night marine air temperature since the late nineteenth century. *J. Geophys. Res. Atmos.* **108**, 4407 (2003).
41. A. Moberg, D. M. Sonechkin, K. Holmgren, N. M. Datsenko, W. Karlén, Highly variable Northern Hemisphere temperatures reconstructed from low- and high-resolution proxy data. *Nature* **433**, 613–617 (2005).
42. M. Rubino, D. M. Etheridge, C. M. Trudinger, C. E. Allison, M. O. Battle, R. L. Langenfelds, L. P. Steele, M. Curran, M. Bender, J. W. C. White, T. M. Jenk, T. Blunier, R. J. Francey, A revised 1000 year atmospheric $\delta^{13}C$-CO_2 record from Law Dome and South Pole, Antarctica. *J. Geophys. Res. Atmos.* **118**, 8482–8499 (2013).
43. C. Bronk Ramsey, Radiocarbon calibration and analysis of stratigraphy: The OxCal program. *Radiocarbon* **37**, 425–430 (1995).
44. C. Bronk Ramsey, Deposition models for chronological records. *Quat. Sci. Rev.* **27**, 42–60 (2008).
45. R. Cember, Bomb radiocarbon in the Red Sea: A medium-scale gas exchange experiment. *J. Geophys. Res.* **94**, 2111–2123 (1989).
46. J. Southon, M. Kashgarian, M. Fontugne, B. Metivier, W. W.-S. Yim, Marine reservoir corrections for the Indian Ocean and Southeast Asia. *Radiocarbon* **44**, 167–180 (2002).
47. S. Kusch, J. Rethemeyer, E. Schefuß, G. Mollenhauer, Controls on the age of vascular plant biomarkers in Black Sea sediments. *Geochim. Cosmochim. Acta* **74**, 7031–7047 (2010).
48. S. Schouten, C. Huguet, E. C. Hopmans, M. V. M. Kienhuis, J. S. Sinninghe Damsté, Analytical methodology for TEX_{86} paleothermometry by high-performance liquid chromatography/atmospheric pressure chemical ionization-mass spectrometry. *Anal. Chem.* **79**, 2940–2944 (2007).
49. G. Trommer, M. Siccha, M. T. J. van der Meer, S. Schouten, J. S. Sinninghe Damsté, H. Schulz, C. Hemleben, M. Kucera, Distribution of Crenarchaeota tetraether membrane lipids in surface sediments from the Red Sea. *Org. Geochem.* **40**, 724–731 (2009).
50. J.-H. Kim, C. Huguet, K. A. F. Zonneveld, G. J. M. Versteegh, W. Roeder, J. S. Sinninghe Damsté, S. Schouten, An experimental field study to test the stability of lipids used for the TEX_{86} and $U^{K'}_{37}$ palaeothermometers. *Geochim. Cosmochim. Acta* **73**, 2888–2898 (2009).
51. S. A. Lincoln, B. Wai, J. M. Eppley, M. J. Church, R. E. Summons, E. F. DeLong, Planktonic Euryarchaeota are a significant source of archaeal tetraether lipids in the ocean. *Proc. Natl. Acad. Sci. U.S.A.* **111**, 9858–9863 (2014).
52. C. Wuchter, S. Schouten, M. J. L. Coolen, J. S. Sinninghe Damsté, Temperature-dependent variation in the distribution of tetraether membrane lipids of marine Crenarchaeota: Implications for TEX_{86} paleothermometry. *Paleoceanography* **19**, PA4028 (2004).
53. S. Schouten, A. Forster, F. E. Panoto, J. S. Sinninghe Damsté, Towards calibration of the TEX_{86} palaeothermometer for tropical sea surface temperatures in ancient greenhouse worlds. *Org. Geochem.* **38**, 1537–1546 (2007).
54. R. Massana, A. E. Murray, C. M. Preston, E. F. DeLong, Vertical distribution and phylogenetic characterization of marine planktonic *Archaea* in the Santa Barbara Channel. *Appl. Environ. Microbiol.* **63**, 50–56 (1997).
55. M. B. Karner, E. F. DeLong, D. M. Karl, Archaeal dominance in the mesopelagic zone of the Pacific Ocean. *Nature* **409**, 507–510 (2001).
56. R. A. Lopes dos Santos, M. Prange, I. S. Castañeda, E. Schefuß, S. Mulitza, M. Schulz, E. M. Niedermeyer, J. S. Sinninghe Damsté, S. Schouten, Glacial–interglacial variability in Atlantic meridional overturning circulation and thermocline adjustments in the tropical North Atlantic. *Earth Planet. Sci. Lett.* **300**, 407–414 (2010).
57. R. Bonnefille, Cenozoic vegetation, climate changes and hominid evolution in tropical Africa. *Global Planet. Change* **72**, 390–411 (2010).
58. S. J. Feakins, N. E. Levin, H. M. Liddy, A. Sieracki, T. I. Eglinton, R. Bonnefille, Northeast African vegetation change over 12 m.y. *Geology* **41**, 295–298 (2013).
59. S. Jung, G. Davies, G. Ganssen, D. Kroon, Stepwise Holocene aridification in NE Africa deduced from dust-borne radiogenic isotope records. *Earth Planet. Sci. Lett.* **221**, 27–37 (2004).
60. D. Sachse, J. Radke, G. Gleixner, Hydrogen isotope ratios of recent lacustrine sedimentary n-alkanes record modern climate variability. *Geochim. Cosmochim. Acta* **68**, 4877–4889 (2004).
61. J. Hou, W. J. D'Andrea, Y. Huang, Can sedimentary leaf waxes record D/H ratios of continental precipitation? Field, model, and experimental assessments. *Geochim. Cosmochim. Acta* **72**, 3503–3517 (2008).
62. D. Sachse, I. Billault, G. J. Bowen, Y. Chikaraishi, T. E. Dawson, S. J. Feakins, K. H. Freeman, C. R. Magill, F. A. McInerney, M. T. J. Van der Meer, P. Polissar, R. J. Robins, J. P. Sachs, H.-L. Schmidt, A. L. Sessions, J. W. C. White, J. B. West, A. Kahmen, Molecular paleohydrology: Interpreting the hydrogen-isotopic composition of lipid biomarkers from photosynthesizing organisms. *Annu. Rev. Earth Planet. Sci.* **40**, 221–249 (2012).
63. M. H. O'Leary, Carbon isotope fractionation in plants. *Phytochemistry* **20**, 553–567 (1981).
64. T. E. Cerling, J. Quade, Y. Wang, J. R. Bowman, Carbon isotopes in soils and palaeosols as ecology and palaeoecology indicators. *Nature* **341**, 138–139 (1989).
65. T. E. Cerling, S. Andanje, D. Kimutai, N. E. Levin, W. D. Mace, A. N. Macharia, B. H. Passey, C. Remien, J. G. Wynn, Paleo-shade: Woody cover, stable isotopes, soil temperature, and soil organic matter in tropical ecosystems. *AGU Fall Meet. Abstr.* **1**, 8 (2010).
66. C. R. Magill, G. M. Ashley, K. H. Freeman, Water, plants, and early human habitats in eastern Africa. *Proc. Natl. Acad. Sci. U.S.A.* **110**, 1175–1180 (2013).
67. R. H. Moss, J. A. Edmonds, K. A. Hibbard, M. R. Manning, S. K. Rose, D. P. van Vuuren, T. R. Carter, S. Emori, M. Kainuma, T. Kram, G. A. Meehl, J. F. B. Mitchell, N. Nakicenovic, K. Riahi, S. J. Smith, R. J. Stouffer, A. M. Thomson, J. P. Weyant, T. J. Wilbanks, The next generation of scenarios for climate change research and assessment. *Nature* **463**, 747–756 (2010).
68. K. Riahi, S. Rao, V. Krey, C. Cho, V. Chirkov, G. Fischer, G. Kindermann, N. Nakicenovic, P. Rafaj, RCP 8.5—A scenario of comparatively high greenhouse gas emissions. *Clim. Change* **109**, 33–57 (2011).
69. S. Fuss, J. G. Canadell, G. P. Peters, M. Tavoni, R. M. Andrew, P. Ciais, R. B. Jackson, C. D. Jones, F. Kraxner, N. Nakicenovic, C. Le Quéré, M. R. Raupach, A. Sharifi, P. Smith, Y. Yamagata, Betting on negative emissions. *Nat. Clim. Chang.* **4**, 850–853 (2014).
70. B. I. Cook, J. E. Smerdon, R. Seager, S. Coats, Global warming and 21st century drying. *Clim. Dyn.* **43**, 1–21 (2014).
71. J. J. Kennedy, N. A. Rayner, R. O. Smith, D. E. Parker, M. Saunby, Reassessing biases and other uncertainties in sea surface temperature observations measured in situ since 1850: 1. Measurement and sampling uncertainties. *J. Geophys. Res. Atmos.* **116**, D14103 (2011).
72. J. J. Kennedy, N. A. Rayner, R. O. Smith, D. E. Parker, M. Saunby, Reassessing biases and other uncertainties in sea surface temperature observations measured in situ since 1850: 2. Biases and homogenization. *J. Geophys. Res. Atmos.* **116**, D14104 (2011).
73. T. M. Smith, R. W. Reynolds, T. C. Peterson, J. Lawrimore, Improvements to NOAA's historical merged land–ocean surface temperature analysis (1880–2006). *J. Clim.* **21**, 2283–2296 (2008).
74. N. H. Saji, B. N. Goswami, P. N. Vinayachandran, T. Yamagata, A dipole mode in the tropical Indian Ocean. *Nature* **401**, 360–363 (1999).

Acknowledgments: We thank K. Anchukaitis and two anonymous reviewers for their comments and input. We acknowledge the World Climate Research Programme's Working Group on Coupled Modelling, which is responsible for CMIP, and the climate modeling groups (listed in table S4) for producing and making their model output available. We thank E. Hamilton, R. Taylor, G. Toltin, J. Donnelly, and S. Madsen for assistance with the laboratory analyses. **Funding:** Funding for this research was provided by the NSF (grant no. OCE-1203892 to J.E.T. and C.C.U.) with contributions from the Center for Climate & Life at Lamont-Doherty Earth Observatory to P.B.D. **Author contributions:** J.E.T., C.C.U., and P.B.D. conceived and designed the study. J.E.T. conducted the organic geochemical and climate model analyses and wrote the paper. C.C.U. assisted with the climate model analyses and interpretation and contributed to the writing of the manuscript. P.B.D. contributed to the paleoclimate data interpretation and writing of the manuscript. **Competing interests:** The authors declare that they have no competing interests.

Data and materials availability: Data associated with this research are available at the National Oceanic and Atmospheric Administration (NOAA) National Climatic Data Center: https://www.ncdc.noaa.gov/paleo/study/19200.

Submitted 27 May 2015
Accepted 20 July 2015
Published 9 October 2015
10.1126/sciadv.1500682

Citation: J. E. Tierney, C. C. Ummenhofer, P. B. deMenocal, Past and future rainfall in the Horn of Africa. *Sci. Adv.* **1**, e1500682 (2015).

Science Advances

Past and future rainfall in the Horn of Africa

Jessica E. Tierney, Caroline C. Ummenhofer and Peter B. deMenocal

Sci Adv **1** (9), e1500682.
DOI: 10.1126/sciadv.1500682